Theoretical Study of the Interaction of NO_2 Molecule with a Metal−Zeolite Model (Metal = Cu, Ag, Au)

Anibal Sierraalta* and Rafael Añez

Laboratorio de Química Computacional, Centro de Química, Instituto Venezolano de Investigaciones Científicas, Apartado 21827, Caracas 1020-A, Venezuela

Marcos-Rosas Brussin

Centro de Catálisis, Petróleo y Petroquímica. Facultad de Ciencias, Universidad Central de Venezuela, Caracas, Venezuela

Received: March 11, 2002

Theoretical calculations of the NO_2 adsorption on transition metal−exchanged zeolite (metal = Cu, Ag, Au) were carried out using density functional theory and MP2 approaches. A tritetrahedral model (T3) was used to represent a fragment of a zeolite. The density functional calculations predict that the NO_2 adsorption energy follows the order: Cu-T3 > Au-T3 > Ag-T3. The analysis of the electronic properties shows that the $d^{10}-s^1d^9$ promotion favors the interaction between the NO_2 molecule and the metallic center. The results show that there is a charge transfer from the metallic ion to the NO_2 molecule, which produces a weakening of the N−O bond. The topology of the laplacian of the density correctly predicts the existence of the two stable isomers found in this work, but not the adsorption order.

Introduction

It is well known that nitrogen oxides, NO_x, are air pollutants that cause photochemical smog and acid rain. Therefore, the reduction of NO_x to N_2 is a very important process in the field of environmental catalysis. Currently, the selective catalytic reduction (SCR) of NO_x with ammonia is the commercial catalytic process for NO_x emission control.[1−4] The reduction is done with NH_3 using titania-supported vanadia in the presence of O_2.[1−4] The main drawback of this process is the handling of ammonia that must be well controlled to avoid the corrosive and toxic effects. Other less aggressive processes such as SCR using hydrocarbons and metal−zeolite exchange, in which ammonia is not used, have been investigated.

From the pioneering works of Iwamoto[5−11] and Held et al.[12] on the reduction of NO_x by hydrocarbons using copper−zeolite catalysts until now, a huge number of works on this topic have been published. The Cu ion-exchanged zeolite catalysts have shown to have good catalytic activities,[13] and some studies have pointed out that the Cu^{1+},[14−18,19] or $Cu^{1+}-Cu^{2+}$ [1−2,20−22] are the active sites of these catalysts. Beside Cu, other systems have been studied too, such as Fe−ZMS-5,[23−29] Co−ZMS-5,[2,9,29−34] Au−MFI,[35,36] or Zn and ZnO.[29,37] Despite all these studies it is not clear yet, for example, which is the oxidation state or the structure of the active site of Fe−ZSM5[25,28] or Cu−zeolite systems.[2,20,22] It is clear that in real catalytic systems there are several cluster species that differ in size and in oxidation state and that are difficult to determine experimentally. Therefore, theoretical studies on adsorption modes, interaction energies, and charge distributions are useful to help to understand the molecular mechanisms of catalytic reduction of NO_x by transition metal−zeolites.

Sauer et al.[18] and Trout[19] have shown that the active site for NO_2 adsorption is a Cu^{1+} species in the Cu−zeolite catalysts. Sodupe and collaborators[38] showed that in gas phase the NO_2 molecule is capable to form stable complexes with silver. Xu[39] reported that at least three stable complexes are possible with gold. Until now, to our knowledge, no theoretical calculations have been performed yet for NO_2 adsorption on silver and gold ion-exchanged zeolites.

In the present work, the bonding of NO_2 on metal-exchanged zeolite (metal = Cu, Ag, and Au) has been investigated by means of quantum chemical calculations. It presents the analysis of the electronic interaction as well as the analysis of the topology of the charge density for the interaction of the NO_2 molecule with a model of metal ion−exchanged zeolite using ab initio density functional theory and MP2 calculations.

Catalyst Model

Three different metal−zeolite (metal = Cu, Ag, and Au) systems were studied in order to analyze the binding energies and electronic properties of the NO_2 adsorbed on a metallic center supported over a zeolite framework. The tritetrahedral structure $[H_3SiOAl(OH)_2OSiH_3]^-$ was chosen to model a T3 site of a zeolite, where the metallic atom, M, was set on bridge between two oxygen atoms (see Figure 1a). Similar models have been used successfully by us[29] and others authors[18,40,41] to represent one of the possible sites of the localization of the metallic ion inside the zeolite framework.

Computational Details

All calculations and geometry optimizations were performed with the Gaussian 94 program[42] at DFT and MP2 level. For DFT, the Becke's three-parameter hybrid functional[43] with Lee, Yang, and Parr correlation functionals were employed.[44] In all cases, the unrestricted formalism (UB3LYP and UMP2) was used. The basis sets and the relativistic compact effective potentials that include explicitly the $(n-1)s^2$, $(n-1)p$,[6] $(n-1)$-

* Corresponding author. E-mail: asierral@ivic.ve.

10.1021/jp0206673 CCC: $22.00
Published on Web 06/26/2002

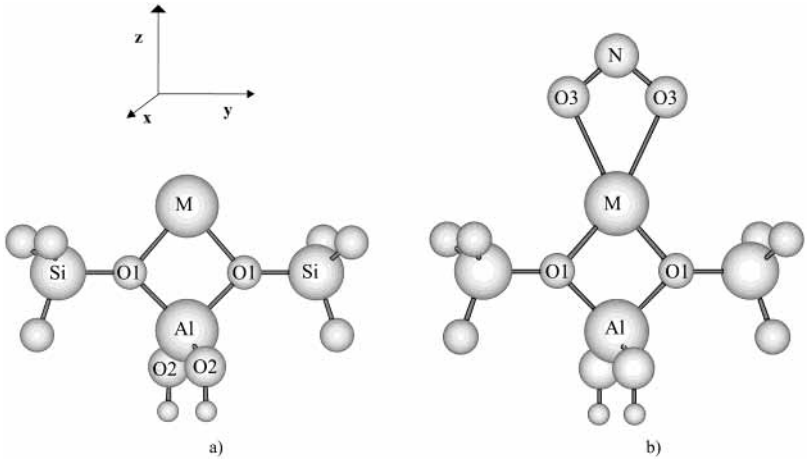

Figure 1. Schematic representation of the molecular structures used in this work. The O1 atoms are localized along the *y* axis. The Al and M atoms are in the *z* axis. (a) M−T3 site (M = Cu, Ag, Au). (b) NO_2M−T3 structure.

d_x, and $(n)s_y$ electrons from Stevens et al.[45] were used for Cu, Ag, and Au atoms. For N and O, the all-electron 6-311G(d, p) basis set was employed. The 6-31G(d, p) basis set was applied to Al, Si, and H atoms. The electronic charge distribution of the catalyst models was analyzed using the natural bond orbital (NBO) partition scheme,[46,47] and the topological properties of the electronic density laplacian was analyzed using the Bubble program. The T3 model (Figure 1a) has a C_{2v} symmetry and the NO_2M−T3 complexes C_2 symmetries (Figure 1b). Only neutral complexes were considered in this work.

Theoretical Background

In the topological theory of Bader "Atoms in a Molecule" (AIM),[48−50] the chemical bonds and molecular reactivity is interpreted in terms of the total molecular electronic density, $\rho(r)$, and its corresponding laplacian, $\nabla^2\rho(r)$. The values of $\rho(r)$ and the $\nabla^2\rho(r)$ at the bond critical point (bcp) allow the characterization of the chemical bonds of the atoms in the molecules. According to the AIM theory, $\nabla^2\rho(r)$ provides information concerning electronic charge. $\nabla^2\rho(r) > 0$ (or $-\nabla^2\rho(r) < 0$) implies locally depleted charge while, on the contrary, $\nabla^2\rho(r) < 0$ (or $-\nabla^2\rho(r) > 0$) signifies locally concentrated charge.[48−49] Thus, classical covalent bonds or shared interactions have values at the bcp of $\nabla^2\rho_{bcp} < 0$ and ρ_{bcp} large, while classical ionic bonds (closed-shell interactions) have $\nabla^2\rho_{bcp} > 0$ and ρ_{bcp} low. Intermediate bonds are associated with $\nabla^2\rho_{bcp} > 0$ and ρ_{bcp} medium or large, i.e.; values between shared and closed-shell. On the other hand, Cremer and Kraka[51,52] have shown that for covalent and intermediate bonds the energy density H_{bcp} has negative values. Another parameter used to describe a bond is the ellipticity (ϵ) that shows if the electronic charge is preferentially accumulated in a given direction between two bonded atoms. Sigma bonds have $\epsilon = 0$, while double or π bonds, in general, have $\epsilon > 0$. Beside the bcp there is another type of critical point (cp) called the ring cp, which is present in ring structures such as benzene, thiophene, etc. It has been proposed[53] that there is a correlation between the interaction energies of some compounds and either $\rho(r)$ or $\nabla^2\rho(r)$ at the ring cp.

The molecular reactivity in the AIM theory is related to the topology of $-\nabla^2\rho(r)$ at the outer valence shell of charge concentration (OVSCC), i.e, with the type and number of critical points of $-\nabla^2\rho(r)$. In the OVSCC, $\rho(r)$ is maximally concentrated and the distribution of $-\nabla^2\rho(r)$ over this surface is, in general, uniform for free atoms. In a molecule, the formation of bonds produces change in the atomic $-\nabla\,^2\rho(r)$, and local maxima, minima, and saddle points appear. There are two important types of critical points of $-\nabla^2\rho(r)$ at the OVSCC: maxima or charge concentrations (cc) and saddle points or electronic holes. The saddle points represent local charge depletions (cd) that are associated with electrophilic sites susceptible to nucleophile attack, while the maxima or cc are associated with the nucleophilic sites susceptible to attack by electrophiles. Thus, the acid−base reaction corresponds to the alignment of a charge concentration in the OVSCC of the base with a charge depletion, or hole, on the acid.[48,49,54]

TABLE 1: Geometry, Charges, Electronic Configuration, and Energy Difference for M−T3(X) Systems (M = Cu, Ag, Au; X = S Singlet, T = Triplet)

method	molecular system	M−O1 Å	angle O1−M−O1	Q_M	total spd configuration	ΔE^a eV
B3LYP	Cu-T3(S)[b]	2.00	83.2	+0.88	$sp^{0.18}\,d^{9.94}$	
B3LYP	Cu-T3(T)	1.98	78.7	+0.74	$sp^{1.09}\,d^{9.17}$	+1.71 (+ 2.42)
B3LYP	Ag-T3(S)	2.27	73.0	+0.87	$sp^{0.16}\,d^{9.97}$	
B3LYP	Ag-T3(T)	2.24	71.4	+0.46	$sp^{1.06}\,d^{9.48}$	+2.88 (+4.84)
B3LYP	Au-T3(S)	2.27	72.4	+0.78	$sp^{0.30}\,d^{9.92}$	
B3LYP	Au-T3(T)	2.25	71.0	+0.51	$sp^{1.16}\,d^{9.33}$	+1.34 (+2.40)
MP2	Cu-T3(S)	1.99	82.6	+0.90	$sp^{0.28}\,d^{9.82}$	
MP2	Cu-T3(T)	1.96	79.7	+0.86	$sp^{1.16}\,d^{8.98}$	+2.70 (+4.08)
MP2	Ag-T3(S)	2.27	72.3	+0.96	$sp^{0.12}\,d^{9.92}$	
MP2	Ag-T3(T)	2.12	73.7	+0.70	$sp^{1.12}\,d^{9.18}$	+3.69 (+5.39)
MP2	Au-T3(S)	2.25	72.3	+0.90	$sp^{0.24}\,d^{9.86}$	
MP2	Au-T3(T)	2.17	72.2	+0.68	$sp^{1.22}\,d^{9.10}$	+1.52 (+2.64)

[a] Values in parentheses correspond to the transition: M^{+1}(singlet) → M^{+1}(triplet) for a single atom. Experimental values: Cu 2.72 eV [64], Ag 4.85 eV [65], Au 1.86 eV [65]. [b] Data from ref 29.

Results and Discussion

Table 1 shows the geometrical properties and the electronic configuration of the M−T3 structures (M= Cu, Ag, and Au) for two spin states (singlet and triplet). In general both methodologies, UB3LYP and UMP2, produce qualitatively the same results. The distance M−O (M−O1, Figure 1a) is shorter for the triplet state than for the singlet, and the positive charge on the metal is greater for the singlet than for the triplet, indicating that one electronic transfer from the metal to the T3 site occurs. The analysis of the electronic configuration of the

TABLE 2: Geometries, Binding Energies (ΔE), and NBO Electronic Populations for NO_2 Metal−T3 Systems [Normal Mode ($NO_2MT3||$)]

molecular system	M−O1 (Å)	angle O1−M−O1	N−O3 (Å)	angle O3−N−O3	O3−M (Å)	ΔE (kcal/mol)
NO_2Cu-T3[a]	1.94	80.6	1.26	110.9	2.02	−43.2
NO_2Ag-T3	2.17	73.2	1.26	111.7	2.23	−7.2
NO_2Au-T3	2.19	72.0	1.26	112.5	2.25	−27.0
NO_2			1.19	134.2		
$NO_2^{(-1)}$			1.26	116.8		

	Q_{NO2}	Q_{metal}	d_{xy}	d_{xz}	d_{yz}	$d_{x^2-y^2}$	d_{z^2}
NO_2Cu-T3[a]	−0.60	+1.33	2.00	1.99	1.31	1.98	1.98
NO_2Ag-T3	−0.50	+1.12	2.00	1.99	1.55	1.99	1.97
NO_2Au-T3	−0.47	+1.06	2.00	1.99	1.44	1.98	1.93

[a] Data from ref 29.

TABLE 3: Geometries, Binding Energies (ΔE), and NBO Electronic Populations for NO_2Metal−T3 Systems [Perpendicular Mode ($NO_2MT3\perp$)

molecular system	M−O1 (Å)	angle O1−M−O1	N−O3 (Å)	angle O3−N−O3	O3−M (Å)	ΔE (kcal/mol)
NO_2Cu-T3[a]	2.00	79.5	1.26	109.9	2.00	−27.9
NO_2Ag-T3	2.26	71.5	1.26	109.4	2.25	+7.8
NO_2Au-T3	2.27	69.7	1.26	110.1	2.23	−7.0

	Q_{NO2}	Q_{metal}	d_{xy}	d_{xz}	d_{yz}	$d_{x^2-y^2}$	d_{z^2}
NO_2Cu-T3[a]	−0.55	+1.34	2.00	1.30	1.98	2.00	1.98
NO_2Ag-T3	−0.35	+1.07	2.00	1.65	1.98	2.00	1.97
NO_2Au-T3	−0.38	+1.07	2.00	1.49	1.96	1.99	1.93

[a] Data from ref 29.

metal shows that in the singlet state the metal has an nd^{10} configuration, while for the triplet, one d electron is promoted to the empty $(n+1)s$ orbital. This promotion reduces the electron−electron repulsion between the electrons of the metal and the electrons of the support reducing therefore, the M−O1 distance.

For the cases presented in Table 1, the transition or promotion energy $nd^{10} \rightarrow nd^9(n+1)s^1$ (singlet to triplet) is lower for the metallic atom anchored on the zeolite than for a single M^+ gas-phase ion. According to the values reported in Table 1, the B3LYP methodology reproduces better the experimental values of the transition energy $M^{+1}(nd^{10}) \rightarrow M^{+1}((n+1)s^1nd^9)$ than does the MP2 approach. This result agrees with the well-known fact that for some transition metals the energies calculated at MPn level are often no reliable.[55,56] For example, for Fe−Cu the Møller−Plesset perturbation energy does not converge and shows large oscillations.[56,57] Our value of 1.7 eV for Cu−T3 is in good agreement with the value reported by Sauer et al.[18] The stabilization of the triplet state by the zeolitic framework is due, in part, to the fact that the $nd^9(n+1)s^1$ promotion reduces the electron−electron repulsion between the metal d electrons and the electrons of the oxygens. Therefore, the electrostatic attraction between the M^+ ion and the T3 site increases, stabilizing the triplet sate and reducing the energy gap.

In both methodologies, DFT and MP2, the highest and the lowest energy gap correspond to the Ag and Au atoms, respectively. Nachtigall, Nachtigallová, and Sauer[41] showed that the values of vertical $T_1 \leftarrow S_0$ excitation energy as well as the vertical $S_0 \leftarrow T_1$ emission energy for Cu^+−zeolite systems depend on the size of the cluster model. Nevertheless, the spread of the values does not exceed the amount of 0.2 eV. Then we expect that the error in our calculations due to the cluster size used be small. Therefore, we can conclude, according to our results, that is easier to produce an electronic excitation on Au-exchanged zeolites than in Cu- or Ag-exchanged zeolites.

Table 2 shows the geometrical properties as well as the calculated binding energy for the normal ($NO_2M-T3||$) adsorption mode of the NO_2 on M−T3 systems (M = Cu, Ag, Au), and Figure 1b displays a schematic representation of the structure of these complexes. In these structures the NO_2 molecule is parallel to the plane O1−Al−O1. All values reported herein for the NO_2M-T3 complexes were obtained using the B3LYP approach.

From the analysis of Table 2 it is clear that the interaction of NO_2 with the metallic atom produces an enlargement of the N−O distance (N−O3) from 1.19 to 1.26 Å and a reduction of the natural angle (O3−N−O3) of the NO_2 molecule. The geometrical parameters of the adsorbed NO_2 are closer to the free ion NO_2^- than to the NO_2 free molecule, which is an indication of a charge transfer from the metal to the NO_2 molecule. The charges and NBO population analysis show that after the interaction of the NO_2 molecule with the M−T3 system, the metallic atom has a d^9 configuration with a high positive charge (+1.33e, +1.12e, +1.06e for M = Cu, Ag, and Au, respectively) with the unpaired electron localized in the nd_{yz} orbital; while the NO_2 is negatively charged. This charge transfer increases the electrostatic interactions of the metal with the negatively charged zeolite, reducing the M−O1 distance and stabilizing the ion. Although there is a charge transfer from the M−T3 system to the NO_2 molecule, calculations with diffuse functions were not performed because previous work[29] showed that neither geometry nor calculated binding energies change significantly when these functions are used.

Table 3 shows the geometrical properties as well as the calculated binding energy for the perpendicular adsorption mode ($NO_2M-T3\perp$). In these structures the NO_2 molecule is perpendicular to the plane O1−Al−O1 and parallel to the plane O2−Al−O2. Again, there is a charge transfer from the metal to the NO_2 molecule and an enlargement of the N−O3 distance and the NBO analysis show that the metal unpaired electron is localized in the nd_{xz} orbital.

TABLE 4: Topological Properties of the Electronic Density[a] of M−T3 and NO_2M−T3 Complexes (M = Cu, Ag, Au)

molecular system	bond	cp type[b]	ρ_{cp}	H_{cp}	$\nabla^2\rho_{cp}$	ϵ
Cu−T3[c]	Cu−O1	bcp	0.0758	−0.0168	0.3865	0.0164
	Cu−O1	bcp	0.0859	−0.0184	0.4313	0.0271
NO_2CuT3||	Cu−O3	bcp	0.0752	−0.0158	0.3266	0.1021
	N−O3	bcp	0.4578	−0.5708	−1.012	0.0841
		ring	0.0441		0.2741	
	Cu−O1	bcp	0.0760	−0.0164	0.3741	0.0544
NO_2CuT3⊥	Cu−O3	bcp	0.0791	−0.0168	0.3492	0.1477
	N−O3	bcp	0.4566	−0.5694	−1.012	0.0886
		ring	0.0455		0.2929	
Ag−T3	Ag−O1	bcp	0.0572	−0.0036	0.2790	0.0389
	Ag−O1	bcp	0.0696	−0.0057	0.3284	0.0276
NO_2Ag T3||	Ag−O3	bcp	0.0640	−0.0045	0.2764	0.1124
	N−O3	bcp	0.4603	−0.5782	−1.025	0.0859
		ring	0.0372		0.2088	
	Ag−O1	bcp	0.0585	−0.0036	0.2902	0.0208
NO_2AgT3⊥	Ag−O3	bcp	0.0613	−0.0035	0.2673	0.1420
	N−O3	bcp	0.4600	−0.5799	−1.033	0.0921
		ring	0.0367		0.1954	
Au−T3	Au−O1	bcp	0.0647	−0.0055	0.2981	0.0433
	Au−O1	bcp	0.0780	−0.0108	0.3345	0.0292
NO_2AuT3||	Au−O3	bcp	0.0712	−0.0076	0.2835	0.1355
	N−O3	bcp	0.4653	−0.5916	−1.055	0.0872
		ring	0.0397		0.2387	
	Au−O1	bcp	0.0655	−0.0057	0.3034	0.0139
NO_2AuT3⊥	Au−O3	bcp	0.0737	−0.0079	0.2979	0.1844
	N−O3	bcp	0.4629	−0.5884	−1.055	0.0961
		ring	0.0410		0.2451	

[a] Values in atomic units. ρ_{cp} electronic density at the cp; H_{cp} energy density at the cp; $\nabla^2\rho_{cp}$ laplacian of $\rho(r)$ at the cp. ϵ bond ellipticity. [b] bcp correspond to a (3, −1) cp; ring type to a (3, +1) cp. [c] Data from ref 29.

The proposed mechanisms[18] to explain the interaction of NO_2 with the metal indicate that the promotion $nd^{10} \rightarrow nd^9(n+1)s^1$ is necessary. In the excited state, d^9s^1, the interaction is done using the s electron of the metal, therefore the unpaired electron must be localized in the d orbitals. For the NO_2M−T3|| complexes, the unpaired electron is localized in the nd_{yz} orbital (see Table 2), while for the NO_2M−T3⊥ the electron is in the nd_{xz} orbital (see Table 3). These results indicate that the promotion must occur in the d orbital that diminishes the electron−electron repulsion between the d electrons of the metallic center and the electrons of the oxygen atoms that belong to the NO_2 molecule. As a matter of fact, the adsorption energy correlates with the electronic population in the nd_{yz} orbital for the NO_2M−T3|| complexes while for NO_2M−T3⊥ the correlation is with the nd_{xz} electronic population, i.e., greater nd_{yz} or nd_{xz} population lowers adsorption energy. Since in the perpendicular mode the nd_{yz} orbital is doubly occupied (see Figure 1b), there is a strong electronic repulsion between the nd_{yz} and the oxygen electrons of the zeolite (atoms O1). This repulsion destabilizes the absorption. Therefore, the binding energies for the NO_2M−T3⊥ are lower than the corresponding to the NO_2M−T3||. The second factor related to the adsorption process is the charge transfer from the metal to the NO_2 molecule. The easier this charge transfer is, the more favored the adsorption process will be. This explains the fact that the binding energy order correlates with the inverse ionization potential order of the M^+ cation; i.e., the binding energy follows the sequence Cu−T3 (IP = 20.3 ev)[58] > Au−T3 (IP = 20.5 ev)[59] > Ag-T3(IP = 21.5 ev).[59]

The topological properties of the molecular electronic density ρ at the bcp, (see Table 4 and Figure 2) show that the interaction between the transition metal (Cu, Ag, and Au) and the oxygen atoms can be classified as closed-shell or intermediate interaction. The molecular electronic density at the bcp (ρ_{bcp}) is low, the lapacian ($\nabla^2\rho_{bcp}$) is positive, but the energy density H_{bcp} has a negative value. Published results[58−61] show that, in general, the metal−oxygen interaction is characterized by positive values of $\nabla^2\rho_{bcp}$ and ϵ. The high ϵ values for M−O3 bonds suggest a strong π contribution in this bond. The values of $\nabla^2\rho$ and ρ at the ring cp predict that for NO_2M−T3|| and NO_2M−T3⊥ complexes the order of the interaction energy is NO_2Cu−T3|| > NO_2Au−T3|| > NO_2Ag−T3|| and NO_2Cu−T3⊥ > NO_2-Au−T3⊥ > NO_2Ag−T3⊥. This is the same order obtained from the calculated binding energies reported in Tables 2 and 3. The trend given by the $\nabla^2\rho$ values or ρ at the ring cp is valid only for the same type of complex; as a matter of fact, the $\nabla^2\rho$ and ρ for NO_2Cu−T3⊥ are greater than for NO_2Cu−T3|| ($\nabla^2\rho$ = 0.2929 au and $\nabla^2\rho$ = 0.2741 au; ρ = 0.0455 au and ρ = 0.0441 au, respectively) but the binding energy is greater for NO_2Cu−T3|| than for NO_2Cu−T3⊥.

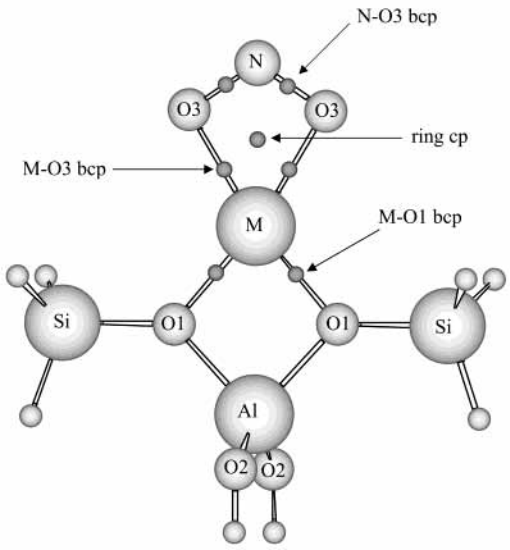

Figure 2. Schematic representation of the position of the critical points (cp) of the electronic density of the NO_2M−T3 structures (M = Cu, Ag, Au). NO_2 is in the plane of the Al and the O1 atoms.

For the M−O3 bonds in the NO_2M−T3 structures (see Table 4), the electronic density ρ_{bcp} correlates with the binding energies only if the same type of complex is used, i.e., greater ρ_{bcp} values correspond to greater binding energies. However, there is not correlation if the values of NO_2M−T3|| and NO_2M−T3⊥ are used in conjunction. For example, for M = Cu and Au, ρ_{bcp}-(NO_2M−T3⊥) > ρ_{bcp}(NO_2M−T3||) but the binding energy ΔE(NO_2M−T3⊥) < ΔE(NO_2M−T3||). This shows that there is not a general correlation between ρ_{bcp} and ΔE.

In the case of the NO_2 and NO_2^- free molecules (see Figure 3), the topological properties of the N−O bond correspond to a shared interaction. The positive values of ϵ can be rationalized considering that the HOMO orbital of these molecules has a strong contribution of the p_z atomic orbital of the N and the O atoms and therefore some π character is present in the N−O bond. Due to the charge transfer from the metal to the NO_2 molecule, the topological properties of the N−O3 bond in the NO_2M−T3 complexes are similar to the properties of the NO_2^- free molecule. The increasing of the N−O bond length in the final complexes NO_2M−T3 (see Tables 2 and 3) results in the electronic density as well as the degree of local charge concentration ($\nabla^2\rho_{bcp}$) being lower than in the NO_2 free molecule and closer to the NO_2^- free molecule.

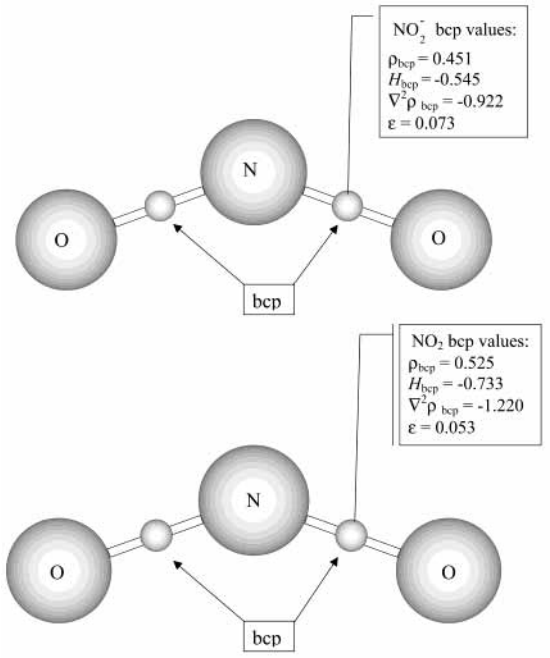

Figure 3. Schematic representation of the position of the critical points of the electronic density and the values of the topological parameter of the NO_2^- ion (top) and the NO_2 neutral molecule (bottom).

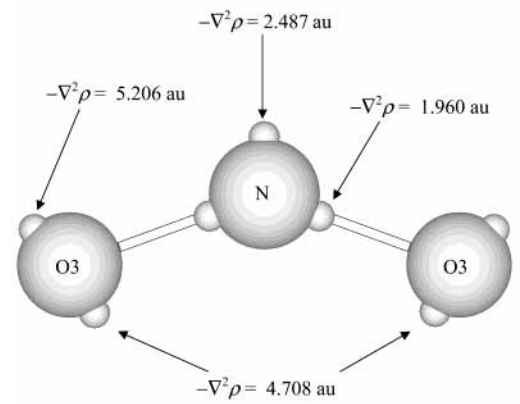

Figure 4. Schematic representation of the positions of the local charge concentrations (lcc's) and the values of $-\nabla^2\rho$ at these points for the NO_2 molecule.

Figure 4 shows the geometric distribution of the local charge concentrations and the values of $-\nabla^2\rho$ at these points for the NO_2 molecule. The OVSCC of the N atom presents three lcc's, two of them in the N−O bond direction, while the oxygen atoms have two lcc's outside the bond area N−O. On the other hand, the M−T3 aggregate shows four lcd's as displayed in Figure 5 and whose values are reported in Table 5. Therefore, it is clear that the reaction of NO_2 with M−T3 corresponds to the alignment of the NO_2 lcc's with the M−T3 lcd's. The values of $-\nabla^2\rho$ at the lcd points of the metallic atoms ($-\nabla^2\rho_L$, $-\nabla^2\rho_X$, see Table 5) correctly predict the stability of the isomers, i.e., $-\nabla^2\rho_L(NO_2M-T3||) > -\nabla^2\rho_X(NO_2M-T3\perp)$ and $\Delta E(NO_2M-T3||) > \Delta E(NO_2M-T3\perp)$ but not the trend $\Delta E(NO_2Cu-T3||) > \Delta E(NO_2Au-T3||) > \Delta E(NO_2Ag-T3||)$.

Conclusions

The geometric parameters, electronic structures, binding energies, and topological properties of the charge distribution have been determined for the M−T3 and NO_2M−T3 systems (M = Cu, Ag, and Au). The results show that the strongest

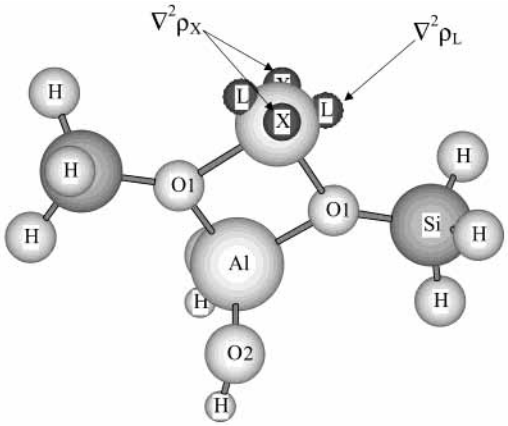

Figure 5. Schematic representation of the position of the local charge depletions, (lcd's), $\nabla^2\rho_L$, and $\nabla^2\rho_X$ in the M−T3 structures (M = Cu, Ag, and Au).

TABLE 5: Values[a] of $-\nabla^2\rho$ and ρ at the Critical Points of $-\nabla^2\rho$ at the Valence Shell of the Metal for the M−T3 Complexes (M= Cu, Ag, Au)

	cp type[b]	ρ_L	$-\nabla^2\rho_L$	ρ_X	$-\nabla^2\rho_X$
Cu−T3	lcd	6.809	126.748	6.624	117.669
Ag−T3	lcd	2.183	30.122	2.168	29.547
Au−T3	lcd	1.634	20.794	1.598	19.549

[a] In atomic units. [b] The lcd type corresponds to (3, +1) cps.

NO_2 interaction corresponds to the Cu atom, while the weakest corresponds to Ag. As a matter of fact, for the perpendicular mode there is not adsorption over the Ag−T3 system. The coordination of NO_2 through the two oxygen atoms to the metallic center was found to be the most stable one, while other coordination modes were found to be less stable. This agrees with previous works[18,38,39,62,63] which show that, in general, the η^2−O,O structure is the most stable one when the NO_2 binds to a metallic ion in a zeolite framework. The lengthening of the N−O bond of the adsorbed NO_2 molecule can be explained in terms of the charge transfer from the M−T3 complex to the nitrogen dioxide. After the interaction, the resulting charge transfer goes to an antibonding NO_2 orbital, weakening the N−O bond. As a matter of fact, the geometrical as well the topological properties of the charge density of the adsorbed NO_2 are closer to the NO_2^- than to the NO_2 free molecule. In addition to this, the increases in the positive charge on the metal favors the electrostatic interactions between the metal and the negatively charged zeolite, therefore reducing the metal−O(ZSM-5) distance.

The bonding mechanism proposed by Sauer et al.[18] explains the interaction of NO_2 with Cu^{1+}, Ag^{1+}, and Au^{1+}. The topology of the laplacian of the electronic density correctly predicts the existence of the two stable isomers found for the NO_2M−T3 systems but not the trend in the binding energy. The binding energy correlates with the values of $\nabla^2\rho$ and ρ at the ring critical point.

Acknowledgment. The authors gratefully acknowledged CONIPET (grant 97003734) and CONICIT (grant S1-96001399) for the financial support. A.S. thanks Prof. Joachim Sauer for helpful discussions during the EuroConference celebrated in San Feliu de Guixols, Spain, June 2001.

References and Notes

(1) Parvulescu, V. I.; Grange, P.; Delmon, B. *Catal. Today* **1998**, *46*, 233.

(2) Bell, A. T. *Catal. Today* **1997**, *38*, 151.
(3) Zhu, Z.; Liu, Z.; Niu, H.; Liu, S.; Hu, T.; Liu, T.; Xie, Y. *J. Catal*. **2001**, *197*, 6.
(4) Maunula, T.; Ahola, J.; Hamada, H. *Appl. Catal. B* **2000**, *26*, 173.
(5) Iwamoto, M.; Furukawa, H.; Mine, Y.; Uemura, F.; Mikuriya, S.; Kagawa, S. *J. Chem. Soc., Chem. Commun.* **1986**, *1272*.
(6) Iwamoto, M.; Furukawa, H.; Kagawa, S. *Stud. Surf. Sci. Catal*. **1986**, *28*, 943.
(7) Iwamoto, M, Yahiro, H.; Mine, Y. *Chem. Lett*. **1989**, *213*.
(8) Iwamoto, M. *Stud. Surf. Sci. Catal*. **1990**, *54*, 121.
(9) Sato, S.; Yu, Y.; Yahiro, H.; Mizuno, N.; Iwamoto, M. *Appl. Catal*. **1991**, *L1*, 70.
(10) Iwamoto, M.; Hamada, S. *Catal. Today* **1991**, *10*, 57.
(11) Iwamoto, M.; Yahiro, H. *Catal. Today* **1994**, *22*, 5.
(12) Held, W.; Koenig, A.; Richter, T.; Puppe, L. *SAE Technol. Paper Ser*. **1990**, *900*, 496.
(13) Shelef, M. *Chem. Rev.* **1995**, *95*, 209.
(14) Iwamoto, M.; Yahiro, H.; Tanda, K.; Mizuno, N.; Mine, Y.; Kagawa, S. *J. Phys. Chem*. **1991**, *95*, 3727.
(15) Li, Y.; Hall, W. K. *J. Catal*. **1991**, *129*, 202.
(16) Spoto, G.; Zecchina, A.; Bordiga, S.; Ricchiardi, G.; Martra, G.; Leofanti, G.; Petrini, G. *Appl. Catal. B* **1994**, *3*, 151.
(17) Wichterlová, B.; Dedecek, J.; Sobalík, J.; Vondrová, Z.; Klier, K. *J. Catal*. **1997**, *169*, 194.
(18) Rodriguez-Santiago, L.; Sierka, M.; Branchadell, V.; Sodupe, M.; Sauer, J. *J. Am. Chem. Soc*. **1998**, *120*, 1545.
(19) Trout, B. L.; Chakraborty, A. K.; Bell, A. T. *J. Phys. Chem*. **1996**, *100*, 17582.
(20) Teraoka, Y.; Tai, C.; Ogawa, H.; Furukawa, H.; Kagawa, S. *Appl. Catal. A* **2000**, *200*, 167.
(21) Centi, G.; Perathoner, S. *Appl. Catal. A* **1995**, *132*, 179.
(22) Torre-Abreu, C.; Henriques, C.; Ribeiro, F. R.; Delahay, G.; Ribeiro, M. F. *Catal. Today* **1999**, *54*, 407.
(23) Lombardo, E.; Sill, G.; D'Itri, J.; Hall, W. K. *J. Catal*. **1998**, *173*, 440.
(24) Feng, X.; Hall, W. K. *J. Catal*. **1997**, *166*, 368.
(25) Joyner, R. W.; Stockernhuber, M. *Catal. Lett.* **1997**, *45*, 15.
(26) Hall, W. K.; Feng, X.; Dumesic, J.; Watwe, R. *Catal. Lett*. **1998**, *52*, 13.
(27) Volodin, A. M.; Sobolev, V. I.; Zhidomirov, G. M. *Kinet. Catal*. **1998**, *39*, 775.
(28) Chen, H. Y.; El-Malki, El-M.; Wang, X.; van Santen, R. A.; Sachtler, W. M. H. *J. Mol. Catal. A* **2000**, *162*, 159.
(29) Sierraalta, A.; Añez, R.; Brussin, M-R. *J. Catal.* **2002**, *205*, 107.
(30) Lukyanov, D.; Lombardo, E.; Sill, G.; D'Itri, J.; Hall, W. K. *J. Catal*. **1996**, *163*, 447.
(31) Lombardo, E.; Sill, G.; D'Itri, J.; Hall, W. K. *J. Catal*. **1998**, *173*, 440.
(32) Li, Y.; Armor, J. N. *Appl. Catal. B* **1993**, *2*, 239.
(33) Li, Y.; Armor, J. N. *Appl. Catal. B* **1992**, *1*, L31.
(34) Li, Y.; Salger, T. L.; Armor, J. N. *J. Catal.* **1994**, *150*, 388.
(35) Salama, T.; Ohnishi, R.; Shido, T.; Ichikawa, M. *J. Catal*. **1996**, *162*, 169.
(36) Salama, T.; Ohnishi, R.; Ichikawa, M. *Chem. Commun*. **1997**, 105.
(37) Rodriguez, J. A.; Jirsak, T.; Dvorak, J.; Sambasivan, S.; Fischer, D. *J. Phys. Chem. B* **2000**, *104*, 319.
(38) Rodríguez-Santiago, L.; Branchadell, V.; Sodupe, M. *J. Chem. Phys.* **1995**, *103*, 9738.
(39) Lu, X.; Xu X.; Wang, N.; Zhang, Q. *J. Phys. Chem. A* **1999**, *103*, 10969.
(40) Solans-Monfort, X.; Branchadell, V.; Sodupe, M. *J. Phys. Chem. A* **2000**, *104*, 3225.
(41) Nachtigall, P.; Nachtigallová, D.; Sauer, J. *J. Phys. Chem. B* **2000**, *104*, 1738.
(42) Frisch, M. J.; Trucks, G. W.; Schlegel, H. B.; Gill, P. M. W.; Johnson, B. G.; Robb, M. A.; Cheeseman, J. R.; Keith, T.; Petersson, G. A.; Montgomery, J. A.; Raghavachari, K.; Al-Laham, M. A.; Zakrzewski, V. G.; Ortiz, J. V.; Foresman, J. B.; Cioslowski, J.; Stefanov, B. B.; Nanayakkara, A.; Challacombe, M.; Peng, C. Y.; Ayala, P. Y.; Chen, W.; Wong, M. W.; Andres, J. L.; Replogle, E. S.; Gomperts, R.; Martin, R. L.; Fox, D. J.; Binkley, J. S.; Defrees, D. J.; Baker, J.; Stewart, J. P.; Head-Gordon, M.; Gonzalez, C.; Pople, J. A. *Gaussian 94*, revision D.4; Gaussian, Inc.: Pittsburgh, PA, 1995.
(43) Becke, A. D. *J. Chem. Phys.* **1993**, *98*, 5648.
(44) Lee, C.; Yang, W.; Parr, R. G. *Phys. Rev. B* **1988**, *37*, 785.
(45) Stevens, W.; Basch, H.; Krauss, M. J. *Chem. Phys*. **1984**, *81*, 6026.
(46) NBO version 3.1; Glendening, E. D., Reed, A. E., Carpenter, J. E., Weinhold, F.
(47) Reed, A. E.; Curtiss, L. A.; Weinhold, F. *Chem. Rev.* **1988**, *88*, 899.
(48) Bader, R. W. F. *Chem. Rev.* **1991**, *91*, 893.
(49) Bader, R. W. F. In *Atoms in Molecules: A Quantum Theory*; Halpern, J., Green, M. L. H., Eds.; Clarendon Press: Oxford, 1990.
(50) Bader, R. W. F.; Essen, H. *J. Chem. Phys*. **1984**, *80*, 1943.
(51) Cremer, D.; Kraka, E. *Angew. Chem., Int. Ed. Engl*. **1984**, *109*, 5917.
(52) Cremer, D.; Kraka, E. *Angew. Chem., Int. Ed. Engl*. **1984**, *23*, 627.
(53) Quiñonero, D.; Frontera, A.; Ballester, P.; Garau, C.; Costa, A.; Deya, P. M. *Chem. Phys. Lett.* **2001**, *339*, 369.
(54) Teruel, H.; Sierraalta, A. *Can. J. Chem*. **1999**, *77*, 1521.
(55) Frenking, G.; Antes, I.; Böhme, M.; Dapprich, S.; Ehlers, A. W.; Jonas, V.; Neuhaus, A.; Otto, M.; Stegmann, R.; Veldkamp, A.; Vyboishchikov, S. F. *Reviews in Computational Chemistry*; Lipkowitz, K. B., Boyd, D. B., Eds.; VCH: New York, 1996; Vol. 8, pp 63−144.
(56) Harrison, J. F. *Chem. Rev*. **2000**, *100*, 679.
(57) Niu, S.; Hall, M. B. *Chem. Rev.* **2000**, *100*, 353.
(58) Kempf, J.; Rohmer, M.; Poblet, J.; Bo, C.; Bénerd, M. *J. Am. Chem. Soc*. **1992**, *114*, 1136.
(59) Gillespie, R.; Bytheway, I.; Tang, T.; Bader, R. F. W. *Inorg. Chem*. **1996**, *35*, 3954.
(60) Sierraalta, A.; Ruette, F. *J. Comput. Chem*. **1994**, *15*, 313.
(61) Sierraalta, A. *Chem. Phys. Lett*. **1994**, *227*, 557.
(62) Rodríguez-Santiago, L.; Solans-Monfort, X.; Sodupe, M.; Branchadell, V. *Inorg. Chem.* **1998**, *37*, 4512.
(63) Rodríguez-Santiago, L.; Sodupe, M.; Branchadell, V. *J. Phys. Chem. A* **1998**, *102*, 630.
(64) Moore, C. E. *Atomic Energy Levels*, United State Department of Commerce, National Bureau of Standards, A. V. Astin Director. Issued August 15, 1952; Vol. II.
(65) Moore, C. E. *Atomic Energy Levels*, United State Department of Commerce, National Bureau of Standards, A. V. Astin Director. Issued May 1, 1958; Vol. III.